# Growth Mechanism of Penniform $BaWO_4$ Nanostructures in Catanionic Reverse Micelles Involving Polymers

**Hongtao Shi, Xiaohong Wang, Nana Zhao, Limin Qi,* and Jiming Ma**

*State Key Laboratory for Structural Chemistry of Unstable and Stable Species, College of Chemistry, Peking University, Beijing 100871, P. R. China*

*Received: August 15, 2005; In Final Form: October 29, 2005*

The formation of penniform $BaWO_4$ nanostructures made of nanowires or nanobelts under the direction of a block copolymer in catanionic reverse micelles has been studied in detail. On the basis of the experimental results obtained from the $BaWO_4$ crystallization in aqueous polymer solutions and careful transmission electron microscopy (TEM) observations of $BaWO_4$ nanostructures formed in reverse micelles containing polymers, a detailed two-stage growth mechanism has been proposed for the formation of the penniform nanostructures in reverse micelles, which involves the polymer-controlled shaft formation (Stage 1) and the mixed surfactants-controlled barb growth (Stage 2). During Stage 1, poly(ethylene glycol)-*block*-poly(methacrylic acid) (PEG-*b*-PMAA) induced the formation of *c*-axis-oriented shuttle-like nanocrystals and the subsequent oriented attachment of these shuttle-like nanocrystals resulted in the formation of [100]-oriented shafts with many parallel [001]-oriented pricks. During Stage 2, [001]-oriented nanowires or nanobelts grew gradually from the pricks into barbs, leading to the formation of well-defined penniform $BaWO_4$ nanostructures with the barb morphology essentially determined by the mixing ratio $r$ of the anionic to cationic surfactants (i.e., nanowires were formed at $r = 1$ while nanobelts were formed at $r$ deviating from 1). The current understanding of the growth mechanism of penniform $BaWO_4$ nanostructures in catanionic reverse micelles involving polymers may be potentially applied for designing a new synthesis system for the controlled synthesis of other hierarchical 1D nanostructures with desired architectures.

## Introduction

One-dimensional (1D) nanostructures, such as nanotubes, nanowires, nanorods, and nanobelts, have been the focus of intense research due to their importance in fundamental research and potential applications in fabrication of nanoscale devices.[1] Recently, many efforts have been devoted to the hierarchical assembly of 1D nanoscale building blocks into ordered superstructures or complex architectures, which is critical for the success of bottom-up approaches toward integrated, functional nanosystems.[2−4] In this regard, ordered nanorod/nanowire arrays have been obtained by the self-assembly of preformed uniform nanorods/nanowires through hydrophobic interaction,[2] entropy-driven ordering,[5] biomolecular recognition process,[6] the Langmuir−Blodgett (LB) technique,[7] and the LB technique coupled with a layer-by-layer process.[8] On the other hand, the self-organized crystal growth of hierarchically ordered, branched architectures made of nanowires/nanobelts has attracted much attention since these nanostructures offer opportunities for increasing structural complexity and enabling greater function,[9] as well as reducing interwire losses associated with assembly of preformed nanowires.[1d] Generally, two different chemical routes have been used for fabricating branched nanowire/nanobelt nanostructures, i.e., gas-phase and solution-phase approaches. Until now, a wide variety of branched nanostructures, such as ZnO nanobridges, nanonails, nanocombs, nanotetrapods, nanopropellers, and nanowire−nanobelt junction arrays,[10] ZnS nanocombs and nanowindmills,[11] hyperbranched Si nanowire structures,[12] and branched GaP nanotrees,[13] have been successfully synthesized by a vapor transport and condensation method. Alternatively, the solution-based approach, which represents a promising route in terms of cost and throughput,[14] has been employed for the synthesis of branched nanostructures including multipods of chalcogenide semiconductors[3,15] and noble metals,[16] snowflakelike $Bi_2S_3$ nanostructures,[17] multiple cone-shaped $BaSO_4$ nanostructures,[18] tree-like $BaCrO_4$ nanobelt structures,[19] and penniform $BaWO_4$ and $BaMoO_4$ nanostructures.[20,21] However, the structural complexity achieved in the branched nanostructures obtained via the solution-phase route is still limited compared with the great success achieved from the gas-phase route. If the mechanisms for solution-based, self-organized growth of hierarchical 1D nanostructures are understood, it could be possible to program the synthesis system to yield complex 1D nanostructures with desired architectures in solution.

As effective colloidal templates or nanostructured reaction media, reverse micelles and microemulsions have been widely used for the controlled synthesis of inorganic nanocrystals with specific size and shape.[2,22] In particular, inorganic nanorods/nanowires of various materials including metals,[23] semiconductors,[24] and barium-containing compounds[25] have been produced in reverse micelles. However, hierarchical architectures made of 1D nanoscale building blocks were not obtained in reverse micelles until recently we reported a unique synthesis of penniform $BaWO_4$ nanostructures made of nanowires in catanionic reverse micelles formed by mixed cationic−anionic surfactants with the assistance of a block copolymer.[20] We have proposed a two-stage growth mechanism for the penniform nanostructures, i.e., the formation of the [100]-oriented shaft

* To whom correspondence should be addressed. E-mail: liminqi@pku.edu.cn.

10.1021/jp0545694 CCC: $33.50 
Published on Web 12/16/2005

**SCHEME 1: Schematic Illustration of the Simplified Formation of Penniform $BaWO_4$ Nanostructures**

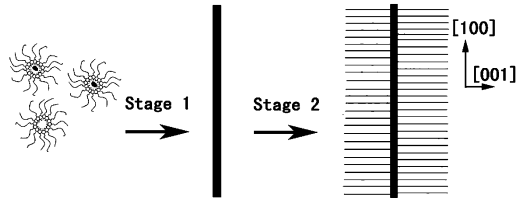


and the subsequent growth of [001]-oriented nanowires perpendicularly on both sides of the shaft in parallel (Scheme 1). However, this tentative growth mechanism is still elusive. For example, it is unclear how the shaft evolves from the primary nanoparticles initially formed in reverse micelles. The exact role played by the polymer PEG-*b*-PMAA (poly(ethylene glycol)-*block*- poly(methacrylic acid)) also remains to be elucidated. Moreover, it is not known whether the penniform $BaWO_4$ nanostructures made of nanobelts can also be prepared with the assistance of the polymer since such nanostructures have been obtained in catanionic reverse micelles with a relatively high mixing ratio ($r$) of the anionic surfactant to the cationic surfactant but without polymers.[21] This work is aimed to address these issues by providing some new experimental evidence and hence to shed light on the growth mechanism.

## Experimental Section

**Materials.** Undecylic acid (99%, Aldrich), decylamine (95%, Aldrich), poly(ethylene glycol)-*block*-poly(methacrylic acid) (PEG-*b*-PMAA, PEG = 3000 g $mol^{-1}$, PMAA = 700 g $mol^{-1}$, Goldschmidt AG), poly(methacrylic acid, sodium salt) (PMAA, $M_w$ = 9500 g $mol^{-1}$, Aldrich), and poly (ethylene glycol) (PEG, $M_w$ = 8000 g $mol^{-1}$, Beijing Chemical Reagents Co.) were used as received. Decane (95%, Beijing Chemical Reagents Co.) was distilled once before used. $Na_2WO_4$ and $BaCl_2$ were of analytical grade and were supplied by Beijing Chemical Reagent Co. The water used was deionized.

**Synthesis.** The polymer-assisted crystallization of $BaWO_4$ was carried out either in aqueous solution or in reverse micelles. For the synthesis of $BaWO_4$ crystals in aqueous solution, 250 $\mu$L of a 0.1 mol $L^{-1}$ $Na_2WO_4$ solution was mixed with 4.5 mL of polymer solution with a certain concentration, which was followed by adding 250 $\mu$L of 0.1 mol $L^{-1}$ $BaCl_2$ with vigorous shaking, giving a reactant concentration of 5 mmol $L^{-1}$. Then, the resultant mixture was incubated at 50 °C for 4 h, resulting in the formation of white precipitates.

The synthesis of penniform $BaWO_4$ nanostructures in reverse micelles was simply achieved by the reaction of the reactant ions solubilized in the aqueous cores of catanionic reverse micelles following the reported procedure.[20] Briefly, 0.782 g of a catanionic surfactant mixture of undecylic acid and decylamine was first dissolved in 2.5 mL of decane under mild heating. Then, 50 $\mu$L of a 0.1 mol $L^{-1}$ $Na_2WO_4$ solution and 100 $\mu$L of a 1 g $L^{-1}$ PEG-*b*-PMAA solution were added with shaking to form a clear solution, which was followed by the addition of 50 $\mu$L of 0.1 mol $L^{-1}$ $BaCl_2$ with vigorous shaking, giving a reactant concentration of 0.025 mol $L^{-1}$ and a polymer concentration of 0.5 g $L^{-1}$ with respect to the aqueous phase of the reverse micelles. Finally, the resultant mixture was incubated at 50 °C for 8 h (unless otherwise stated), resulting in the formation of white precipitates.

**Characterization.** The products were collected, washed with ethanol, and characterized by transmission electron microscopy (TEM, JEOL JEM-200CX, 160 kV), scanning electron microscopy (SEM, FEI STRATA DB235, 10 kV), and X-ray diffraction (XRD, Rigaku Dmax-2000, Cu K$\alpha$ radiation).

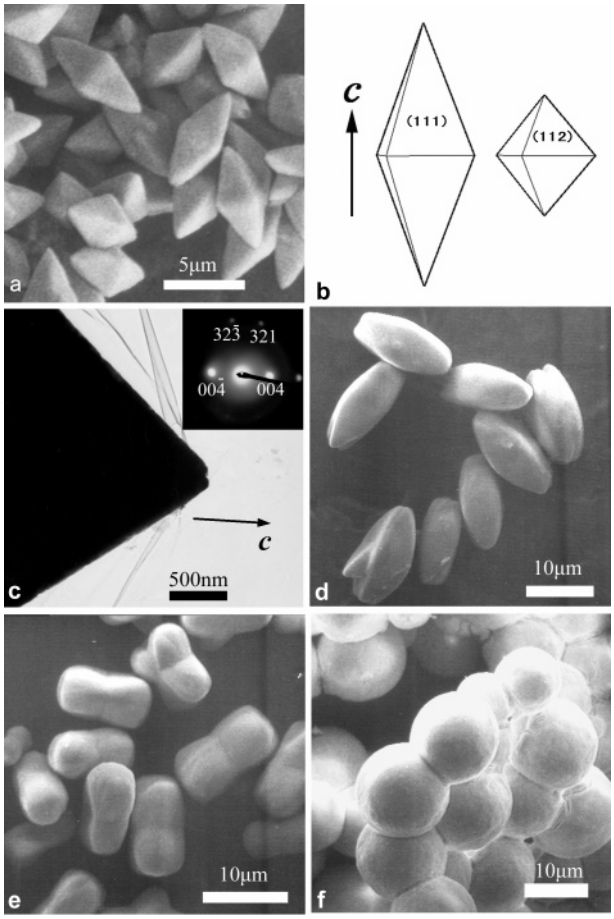


**Figure 1.** SEM (a, d−f) and TEM (c) images of $BaWO_4$ particles obtained in aqueous solution in the presence of PEG-*b*-PMAA and a schematic illustration of bipyramidal $BaWO_4$ crystals (b). The inset shows the ED pattern corresponding to the tip of a bipyramidal crystal. [PEG-*b*-PMAA]: (a, c) 0, (d) 0.2, (e) 0.4, and (f) 0.8 g $L^{-1}$.

## Results and Discussion

The $BaWO_4$ crystallization was first performed in aqueous solution at 50 °C in the presence of the block copolymer PEG-*b*-PMAA to examine the effect of the polymer as an additive on the crystallization of $BaWO_4$ crystals. Figure 1 shows the SEM images of the $BaWO_4$ crystals obtained at different PEG-*b*-PMAA concentrations. It can be seen that bipyramidal crystals with a 4-fold symmetry characteristic of the tetragonal crystal structure were obtained in the absence of the polymer (Figure 1a). The well-defined bipyramidal morphology is characteristic of single-crystalline tetragonal $BaWO_4$ crystals bound by 8 planes of {11$l$}, e.g., {111} and {112}, and elongated along the $c$ axis (Figure 1b). Figure 1c shows the selective area electron diffraction pattern (ED) corresponding to the tip of a bipyramidal crystal, which confirms that the bipyramid is actually elongated along the $c$ axis. The corresponding XRD pattern (Figure 2a) exhibits sharp diffraction peaks attributed to the tetragonal scheelite structure of $BaWO_4$ (JCPDS card 43-0646: $a$ = 0.561 nm, $c$ = 1.270 nm), confirming the formation of tetragonal $BaWO_4$ bipyramids. The addition of 0.2 g $L^{-1}$ of PEG-*b*-PMAA to the solution resulted in the formation of *c*-axis-elongated shuttle-like particles (Figure 1d). When the PEG-*b*-PMAA concentration was increased to 0.4 g $L^{-1}$, nonfaceted peanut-like particles were obtained (Figure 1e). The peanuts

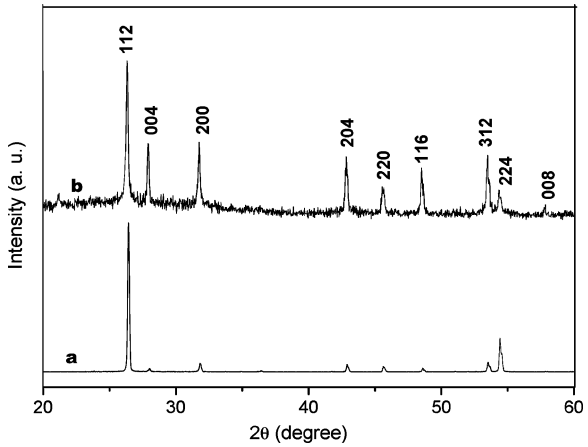


**Figure 2.** XRD patterns of $BaWO_4$ particles obtained in aqueous solution in the presence of PEG-*b*-PMAA. [PEG-*b*-PMAA]: (a) 0 and (b) 0.8 g $L^{-1}$.

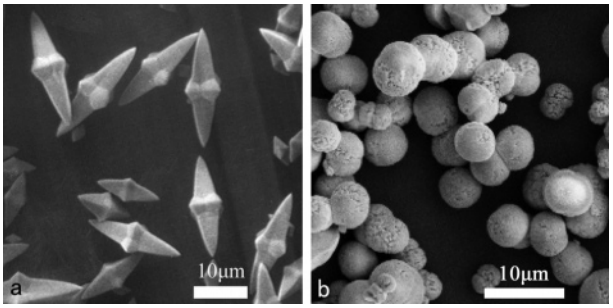


**Figure 3.** SEM images of $BaWO_4$ particles obtained in aqueous solution in the presence of 1.0 g $L^{-1}$ of PEG (a) and 0.2 g $L^{-1}$ of PMAA (b).

evolved into spherical particles with further increasing the polymer concentration to 0.8 g $L^{-1}$ (Figure 1f), which were also revealed to be $BaWO_4$ crystals of the tetragonal scheelite structure by the related XRD pattern (Figure 2b). These results suggest that PEG-*b*-PMAA can considerably influence the $BaWO_4$ crystallization by weakening the anisotropic growth and smoothing the faceted surface. For comparison purposes, the $BaWO_4$ crystallization was also carried out in the presence of two homopolymers PEG and PMAA. As shown in Figure 3, the effect of PEG was relatively weak, leading to the formation of $BaWO_4$ crystals with a partly deformed bipyramidal morphology even at a high concentration of 1.0 g $L^{-1}$ whereas the effect of PMAA was significant, resulting in the formation of spherical $BaWO_4$ crystals even at a low concentration of 0.2 g $L^{-1}$. The obtained results suggest that the PMAA block of the copolymer PEG-*b*-PMAA can interact strongly with the growing $BaWO_4$ crystals through nonspecific adsorption on the crystal surfaces while the PEG block interacts just weakly with the growing crystals and mainly promotes solubilization in water, characteristic of the so-called double-hydrophilic block copolymers (DHBCs).[26] It is indicated that PEG-*b*-PMAA could induce the formation *c*-axis-oriented shuttle-like $BaWO_4$ crystals in aqueous solution; nevertheless, it remains unclear how the *a*-axis-oriented rodlike shaft formed under the direction of PEG-*b*-PMAA in reverse micelles.

As demonstrated previously, bundles of single-crystalline $BaWO_4$ nanowires ~3.5 nm in diameter grown along the [001]-direction were obtained in catanionic reverse micelles with an equimolar mixing ratio ($r = 1$) without polymer.[25e] The addition of 0.5 g $L^{-1}$ of PEG-*b*-PMAA to the aqueous phase of the reverse micelle system resulted in the formation of penniform $BaWO_4$ nanostructures consisting of an *a*-axis-oriented shaft

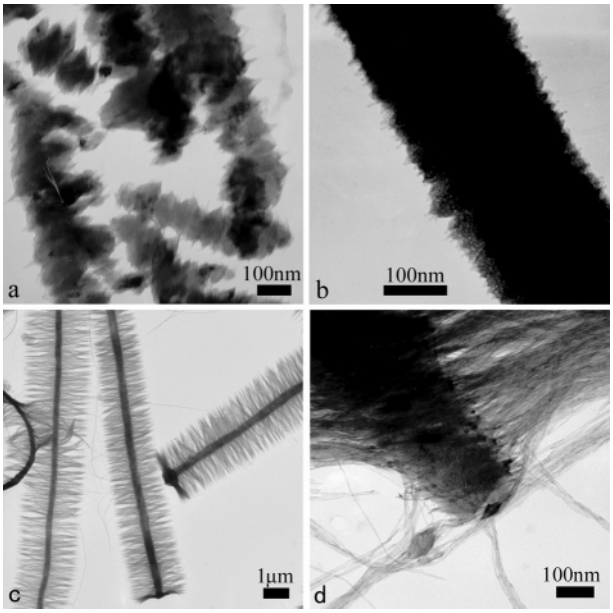


**Figure 4.** TEM images of $BaWO_4$ nanostructures formed in reverse micelles with $r = 1$ in the presence of 0.5 g $L^{-1}$ of PEG-*b*-PMAA after different periods of aging time. Aging time: (a) 10 min; (b) 20 min; and (c, d) 24 h.

200−400 nm in width and many [001]-oriented nanowires ~3.5 nm in diameter grown perpendicularly on both sides of the shaft.[20] Although it was observed that the side nanowires or barbs grew gradually from about 200 nm to more than 2 $\mu$m with increasing aging time from 30 min to 8 h and a two-stage growth mechanism (Scheme 1) was proposed accordingly, it was unknown how the shaft formed under the direction of the polymer. We have carefully examined the earlier stages of the shaft formation and found that the shaft was actually formed by oriented attachment of preformed shuttle-like nanocrystals. As shown in Figure 4a, rudimentary shafts assembled by the attachment of parallel aligned, *c*-axis-oriented shuttle-like particles about 80−200 nm in length were obtained after 10 min of aging. These shuttle-like $BaWO_4$ nanocrystals are reminiscent of the shuttle-like crystals obtained in aqueous PEG-*b*-PMAA solution (Figure 1d) although there is a significant difference in the crystal size, indicating that the presence of PEG-*b*-PMAA in reverse micelles might also induce the formation of the shuttle-like crystals while the reverse-micelle medium greatly limited the crystal size. With increasing aging time to 20 min, the rudimentary shafts evolved into mature shafts, which were typically larger than 200 nm in width and showed a relatively compact interior and a rough surface with many short pricks extruding toward both sides (Figure 4b). This result strongly indicates that the *a*-axis-oriented shafts formed by oriented attachment and fusion of preformed *c*-axis-oriented shuttle-like $BaWO_4$ nanocrystals along the [100] axis of the scheelite lattice. It is noted that the oriented attachment mechanism originally put forward by Penn and Banfield[27] has been applied to explain the anisotropic growth of a variety of nanorods/nanowires via self-assembly of quasispherical nanocrystals.[28] The current formation of the $BaWO_4$ shafts via self-assembly of shuttle-like nanocrystals may represent another example of the oriented attachment. The inherent crystal structural anisotropy or dipolar interaction, as well as crystal surface reactivity, was identified in previous studies as the driving force for the 1D growth via oriented attachment. Considering that the phenomenon of self-assembly of nanorods via lateral attachment into chainlike or ribbonlike structure has

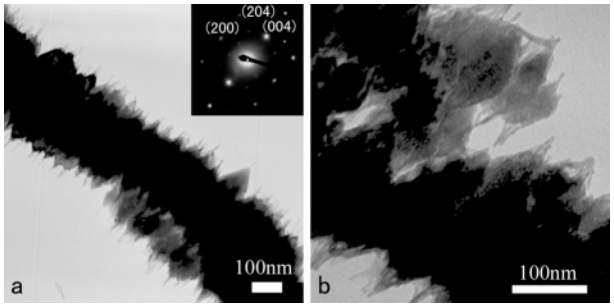


**Figure 5.** TEM images of $BaWO_4$ nanostructures formed in reverse micelles with $r = 1$ in the presence of 0.6 g $L^{-1}$ of PEG-*b*-PMAA. The inset shows the related ED pattern.

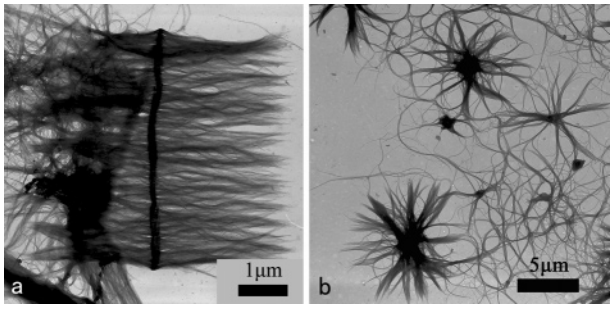


**Figure 6.** TEM images of $BaWO_4$ nanostructures formed in reverse micelles with $r = 1$ in the presence of 1.0 g $L^{-1}$ of PEG (a) and 0.6 g $L^{-1}$ of PMAA (b).

been previously observed,[2,5] it may be rationally suggested that the morphological anisotropy of the shuttle-like crystals, in addition to the inherent anisotropy of the tetragonal crystal structure, contributes largely to the driving force for the 1D growth of the current $BaWO_4$ shafts.

Another piece of evidence that supports the oriented attachment mechanism came from our TEM observation of the penniform $BaWO_4$ nanostructures obtained after 24 h of aging. Figure 4c shows a typical overview image of the well-developed penniform nanostructures, which is very similar to the product obtained after 8 h of aging,[20] suggesting that the penniform nanostructures essentially remained unchanged after growing for 8 h. However, an enlarged image of the end of the shaft reveals that a few shuttle-like particles at the shaft tip did not coalesce well to the shaft and a shuttle-like particle with nanowires grown from both its tips even departed from the shaft (Figure 4d). Moreover, there was a tendency that the length of the side nanowires of the penniform nanostructures was decreased with increasing the PEG-*b*-PMAA concentration in the reverse micelles. It was frequently observed that at a slightly higher PEG-*b*-PMAA concentration (0.6 g $L^{-1}$), only short pricks were grown on both sides of the shaft even after 8 h of aging in reverse micelles (Figure 5a). The related electron diffraction (ED) pattern exhibited clear spots indexed to tetragonal $BaWO_4$ of the scheelite structure, indicating that the prickly shaft was single-crystal elongated along the [100] axis and the short pricks were [001]-oriented. A closer observation of the shafts also revealed that the shaft was assembled by oriented aggregation of shuttle-like nanocrystals (Figure 5b). On the basis of these observations, it may be concluded that the shaft of the penniform $BaWO_4$ nanostructures actually evolved from the oriented attachment of the primary shuttle-like $BaWO_4$ nanocrystals and the presence of the polymer PEG-*b*-PMAA played a key role in the formation of these shuttle-like nanocrystals as well as the shaft formation. In other words,

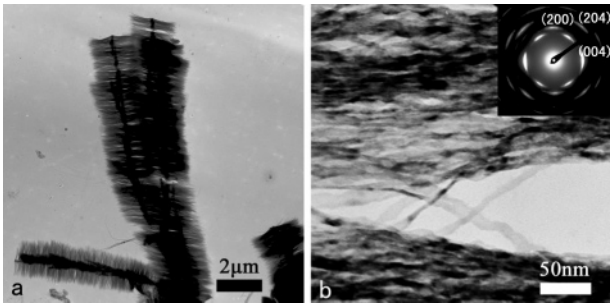


**Figure 7.** TEM images of penniform $BaWO_4$ nanostructures formed in reverse micelles with $r = 1.2$ in the presence of 0.8 g $L^{-1}$ of PEG-*b*-PMAA. The inset shows the related ED pattern.

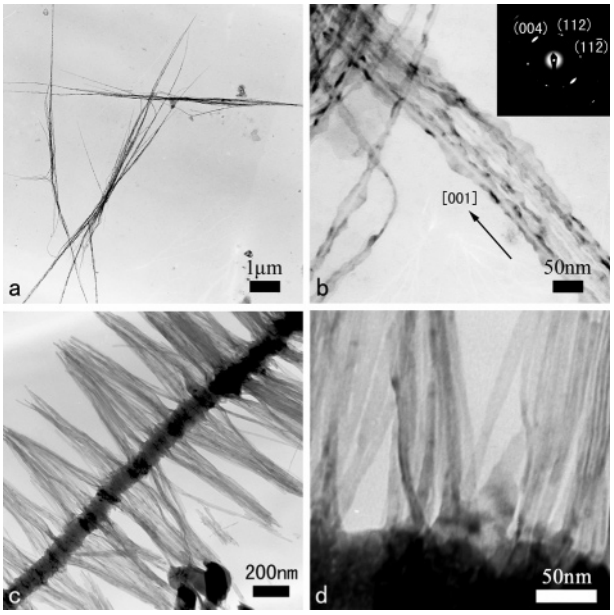


**Figure 8.** TEM images of $BaWO_4$ nanostructures formed in reverse micelles with $r = 0.4$ in the presence of PEG-*b*-PMAA. [PEG-*b*-PMAA]: (a, b) 0 and (c, d) 0.4 g $L^{-1}$. The inset shows the related ED pattern.

the presence of PEG-*b*-PMAA is a predominant factor in the first stage of the formation of the penniform nanostructures.

For comparison purposes, the synthesis of $BaWO_4$ nanostructures in reverse micelles was also performed in the presence of the homopolymers PEG and PMAA. In the presence of 1.0 g $L^{-1}$ of PEG, bundles of nanowires were the predominant product but penniform nanostructures occasionally can be observed (Figure 6a). When the PEG concentration was varied in the range from 0.4 to 10 g $L^{-1}$, this situation did not change significantly. On the other hand, the presence of 0.6 g $L^{-1}$ of PMAA in the reverse micelles induced the formation of starlike nanostructures instead of penniform nanostructures (Figure 6b). No penniform nanostructures were observed when the PMAA concentration was varied in a wide range (0.1−5 g $L^{-1}$). This result suggests that the nonspecific interaction of PMAA with the growing $BaWO_4$ crystals was too strong, which would favor the formation of spherical particles rather than shuttle-like particles, resulting in the disappearance of shafts assembled by shuttle-like nanocrystals. In the case of PEG, there existed a certain degree of weak interaction between PEG and the growing $BaWO_4$ crystals, which led to the formation of a mall number of shuttle-like nanocrystals and hence a few shafts, resulting in the formation of penniform nanostructures as a minority product. Therefore, the copolymer PEG-*b*-PMAA containing both PEG and PMAA blocks could exhibit an appropriate interaction with

**SCHEME 2: Schematic Illustration of the Detailed Formation of Penniform $BaWO_4$ Nanostructures**

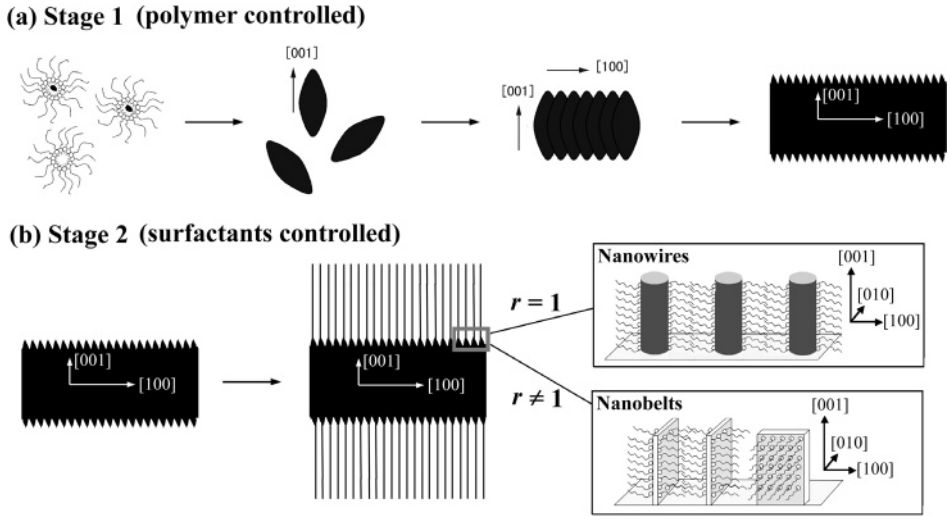


the growing $BaWO_4$ crystals and so acted as a suitable additive for the formation of pure penniform $BaWO_4$ nanostructures in the catanionic reverse micelles.

The second stage of the formation of penniform $BaWO_4$ nanostructures involved the gradual growth of $BaWO_4$ nanowires ~3.5 nm in diameter perpendicularly on both sides of the prickly shafts. Since the same nanowires can form in the reverse micelles without PEG-*b*-PMAA, the role played by PEG-*b*-PMAA seemed to diminish significantly in this stage possibly due to the decrease in the polymer concentration in solution resulting from the adsorption of most PEG-*b*-PMAA molecules on the shafts formed during the first stage. In other words, the mixed surfactants could play a dominant role in the second stage of the formation of the penniform nanostructures. In that case, the morphology of the barbs of the feathers would be controlled by the molar ratio ($r$) of the anionic surfactant to the cationic surfactant in the reverse micelles, which has been demonstrated to be a key factor in determining the morphology of 1D $BaWO_4$ nanostructures.[21] For example, [001]-oriented $BaWO_4$ nanowires were obtained in the reverse micelles with $r = 1$ whereas $BaWO_4$ nanobelts grown along the [001] direction with the top (100) surface tended to form in the reverse micelles with $r$ deviating from 1. In particular, bundles of $BaWO_4$ nanobelts were produced in the reverse micelles with $r = 1.2$.[21] Therefore, an experiment was carried out in reverse micelles with $r = 1.2$ in the presence of PEG-*b*-PMAA and the obtained $BaWO_4$ nanostructures were shown in Figure 7. As expected, penniform nanostructures consisting of [001]-oriented $BaWO_4$ nanobelts grown perpendicularly on both sides of a shaft were obtained, confirming the determining role of the $r$ value on the barb morphology. Notably, it was reported that penniform $BaWO_4$ nanostructures made of nanobelts were also obtained at a larger $r$ value ($r = 1.35$) even without PEG-*b*-PMAA.[21] This result implied that in the case of a larger excess of undecylic acid with respect to decylamine, the excess undecylic acid could act as an additive like PEG-*b*-PMAA to induce the shaft formation prior to the nanobelt formation, leading to the final formation of penniform nanostructures made of nanobelts.

It is worth noting that penniform $BaWO_4$ nanostructures made of nanobelts can also be prepared in reverse micelles with $r < 1$ in the presence of PEG-*b*-PMAA while these nanostructures cannot be obtained without PEG-*b*-PMAA at $r < 1$ where the decylamine is in excess. To illustrate, $BaWO_4$ nanobelts grown along the [001] axis were produced at $r = 0.4$ in the absence of PEG-*b*-PMAA (Figure 8a,b). After the addition of 0.4 g $L^{-1}$ of PEG-*b*-PMAA, penniform $BaWO_4$ nanostructures with uniform nanobelts grown perpendicularly on both sides of the shaft were produced (Figure 8c,d). It is noted that the [001]-oriented nanobelts were grown with their top surface randomly perpendicular to or parallel to the shaft direction, i.e., the [100] direction, since the (100) and (010) surfaces are actually equivalent crystal surfaces belonging to the {100} planes of the tetragonal structure. This result provides further support for the conclusion that PEG-*b*-PMAA played a key role in the shaft formation while the mixed surfactants largely controlled the subsequent growth of nanowires or nanobelts on the shafts.

## Conclusions

The growth of penniform $BaWO_4$ nanostructures under the direction of the block copolymer PEG-*b*-PMAA in catanionic reverse micelles has been carefully studied and a detailed two-stage growth mechanism (Scheme 2) has been proposed based on the experimental observations. The formation of the penniform nanostructures is divided into two growth stages, i.e., the polymer-controlled shaft formation (Stage 1) and the mixed surfactants-controlled barb growth (Stage 2). During Stage 1, the polymer PEG-*b*-PMAA participated in the precipitation process of $BaWO_4$ in aqueous cores of catanionic reverse micelles and induced the formation of *c*-axis-oriented shuttle-like nanocrystals. Then, the side-by-side assembly and fusion of the shuttle-like nanocrystals via oriented attachment along the [100] direction resulted in the formation of [100]-oriented prickly shafts with many [001]-oriented pricks grown perpendicularly on both sides of the shaft in parallel. The gradual adsorption of PEG-*b*-PMAA molecules on the growing shafts would lead to a considerable decrease of the concentration of free polymer molecules in solution, which could finally result in the transition of the crystal growth process from Stage 1 to Stage 2 due to the low polymer concentration in solution. During Stage 2, [001]-oriented nanowires or nanobelts grew gradually from the pricks at approximately equal growth rates, leading to the formation of well-defined penniform $BaWO_4$ nanostructures. The morphology of the feather barbs was essentially determined by the mixing ratio $r$ of the anionic to cationic surfactants, i.e., [001]-oriented nanowires were formed at $r = 1$ while [001]-oriented nanobelts with the (100) top surface either perpendicular or parallel to the [100] direction of the shaft were formed at $r$ deviating from 1. The current understanding of the growth mechanism of penniform $BaWO_4$ nanostructures in catanionic

reverse micelles involving polymers may be potentially applied for designing a new synthesis system for the controlled synthesis of other hierarchical 1D nanostructures with desired architectures.

**Acknowledgment.** This work was supported by the National Natural Science Foundation of China (20325312, 20473003, 20233010) and the Foundation for the Author of National Excellent Doctoral Dissertation of China (200020).

## References and Notes

(1) (a) Hu, J.; Odom, T. W.; Lieber, C. M. *Acc. Chem. Res.* **1999**, *32*, 435. (b) Xia, Y.; Yang, P.; Sun, Y.; Wu, Y.; Mayers, B.; Gates, B.; Yin, Y.; Kim, F.; Yan, H. *Adv. Mater.* **2003**, *15*, 353. (c) Wang, Z. L. *Annu. Rev. Phys. Chem.* **2004**, *55*, 159. (d) Sirbuly, D. J.; Law, M.; Yan, H.; Yang, P. *J. Phys. Chem. B* **2005**, *109*, 15190.

(2) Li, M.; Schnablegger, H.; Mann, S. *Nature* **1999**, *402*, 393.

(3) (a) Manna, L.; Milliron, D. J.; Meidel, A.; Scher, E. C.; Alivisatos, A. P. *Nat. Mater.* **2003**, *2*, 382. (b) Milliron, D. J.; Hughes, S. M.; Cui, Y.; Manna, L.; Li, J.; Wang, L.; Alivisatos, A. P. *Nature* **2004**, *430*, 190.

(4) (a) Kovtyukhova, N. I.; Mallouk, T. E. *Chem. Eur. J.* **2002**, *8*, 4354. (b) Yang, P. *MRS Bull.* **2005**, *30*, 85.

(5) Jana, N. R. *Angew. Chem., Int. Ed.* **2004**, *43*, 1536.

(6) (a) Dujardin, E.; Hsin, L.-B.; Wang, C. R. C.; Mann, S. *Chem. Commun.* **2001**, 1264. (b) Caswell, K. K.; Wilson, J. N.; Bunz, U. H. F.; Murphy, C. J. *J. Am. Chem. Soc.* **2003**, *125*, 13914.

(7) (a) Kim, F.; Kwan, S.; Akana, J.; Yang, P. *J. Am. Chem. Soc.* **2001**, *123*, 4360. (b) Tao, A.; Kim, F.; Hess, C.; Goldberger, J.; He, R.; Sun, Y.; Xia, Y.; Yang, P. *Nano Lett.* **2003**, *3*, 1229.

(8) Whang, D.; Jin, S.; Wu, Y.; Lieber, C. M. *Nano Lett.* **2003**, *3*, 1255.

(9) Wang, D.; Lieber, C. M. *Nat. Mater.* **2003**, *2*, 355.

(10) (a) Lao, J. Y.; Wen, J. G.; Ren, Z. F. *Nano Lett.* **2002**, *2*, 1287. (b) Lao, J. Y.; Huang, J. Y.; Wang, D. Z.; Ren, Z. F. *Nano Lett.* **2003**, *3*, 235. (c) Yan, H.; He, R.; Johnson, J.; Law, M.; Saykally, R. J.; Yang, P. D. *J. Am. Chem. Soc.* **2003**, *125*, 4728. (d) Yan, H.; He, R.; Pham, J.; Yang, P. *Adv. Mater.* **2003**, *15*, 402. (e) Gao, P. X.; Wang, Z. L. *Appl. Phys. Lett.* **2004**, *84*, 2883. (f) Gao, P.; Wang, Z. L. *J. Phys. Chem. B* **2002**, *106*, 12653.

(11) Ma, C.; Moore, D.; Li, J.; Wang, Z. L. *Adv. Mater.* **2003**, *15*, 228.

(12) Wang, D.; Qian, F.; Yang, C.; Zhong, Z.; Lieber, C. M. *Nano Lett.* **2004**, *4*, 871.

(13) Dick, K. A.; Deppert, K.; Larsson, M. W.; Martensson, T.; Seifert, W.; Wallenberg, L. R.; Samuelson, L. *Nat. Mater.* **2004**, *3*, 380.

(14) Sun, Y.; Mayers, B.; Herricks, T.; Xia, Y. *Nano Lett.* **2003**, *3*, 955.

(15) (a) Peng, Z. A.; Peng, X. *J. Am. Chem. Soc.* **2002**, *124*, 3343. (b) Jun, Y.-w.; Lee, S.-M.; Kang, N.-J.; Cheon, J. *J. Am. Chem. Soc.* **2001**, *123*, 5150. (c) Jun, Y.-w.; Jung, Y.-y.; Cheon, J. *J. Am. Chem. Soc.* **2002**, *124*, 615. (d) Lee, S.-M.; Jun, Y.-w.; Cho, S.-N.; Cheon, J. *J. Am. Chem. Soc.* **2002**, *124*, 11244.

(16) (a) Chen, S.; Wang, Z. L.; Ballato, J.; Foulger, S. H.; Carroll, D. L. *J. Am. Chem. Soc.* **2003**, *125*, 16186. (b) Sau, T. K.; Murphy, C. J. *J. Am. Chem. Soc.* **2004**, *126*, 8648. (c) Hao, E.; Bailey, R. C.; Schatz, G. C.; Hupp, J. T.; Li, S. *Nano Lett.* **2004**, *4*, 327. (d) Teng, X.; Yang, H. *Nano Lett.* **2005**, *5*, 885.

(17) Lu, Q.; Gao, F.; Komarneni, S. *J. Am. Chem. Soc.* **2004**, *126*, 54.

(18) (a) Qi, L.; Cölfen, H.; Antonietti, M.; Li, M.; Hopwood, J. D.; Ashley, A. J.; Mann, S. *Chem. Eur. J.* **2001**, *7*, 3526. (b) Yu, S. H.; Antonietti, M.; Cölfen, H.; Hartmann, J. *Nano Lett.* **2003**, *3*, 379.

(19) Shi, H.; Qi, L.; Ma, J.; Cheng, H.; Zhu, B. *Adv. Mater.* **2003**, *15*, 1647.

(20) Shi, H.; Qi, L.; Ma, J.; Cheng, H. *J. Am. Chem. Soc.* **2003**, *125*, 3450.

(21) Shi, H.; Qi, L.; Ma, J.; Wu, N. *Adv. Funct. Mater.* **2005**, *15*, 442.

(22) (a) Pileni, M. P. *Nat. Mater.* **2003**, *2*, 145. (b) Burda, C.; Chen, X.; Narayanan, R.; El-Sayed, M. A. *Chem. Rev.* **2005**, *105*, 1025.

(23) Lisiecki, I. *J. Phys. Chem. B* **2005**, *109*, 12231.

(24) Simmons, B. A.; Li, S.; John, V. T.; McPherson, G. L.; Bose, A.; Zhou, W.; He, J. *Nano Lett.* **2002**, *2*, 263.

(25) (a) Qi, L. M.; Ma, J. M.; Cheng, H. M.; Zhao, Z. G. *J. Phys. Chem. B* **1997**, *101*, 3460. (b) Hopwood, J. D.; Mann, S. *Chem. Mater.* **1997**, *9*, 1819. (c) Li, M.; Mann, S. *Langmuir* **2000**, *16*, 7088. (d) Kwan, S.; Kim, F.; Akana, J.; Yang, P. D. *Chem. Commun.* **2001**, 447. (e) Shi, H.; Qi, L.; Ma, J.; Cheng, H. *Chem. Commun.* **2002**, 1704.

(26) Cölfen, H. *Macromol. Rapid Commun.* **2001**, *22*, 219.

(27) (a) Penn, R. L.; Banfield, J. F. *Science* **1998**, *281*, 969. (b) Penn, R. L.; Banfield, J. F. *Geochim. Cosmochim. Acta* **1999**, *63*, 1549. (c) Banfield, J. F.; Welch, S. A.; Zhang, H.; Ebert, T. T.; Penn, R. L. *Science* **2000**, *289*, 751. (d) Alivisatos, A. P. *Science* **2000**, *289*, 736.

(28) (a) Pacholski, C.; Kornowski, A.; Weller, H. *Angew. Chem., Int. Ed.* **2002**, *41*, 1188. (b) Lu, W.; Gao, P.; Jian, W. B.; Wang, Z. L.; Fang, J. *J. Am. Chem. Soc.* **2004**, *126*, 14816. (c) Cho, K.-S.; Talapin, D. V.; Gaschler, W.; Murray, C. B. *J. Am. Chem. Soc.* **2005**, *127*, 7140. (d) Yu, J. H.; Joo, J.; Par, H. M.; Baik, S.-I.; Kim, Y. W.; Kim, S. C.; Hyeon, T. *J. Am. Chem. Soc.* **2005**, *127*, 5662.